Regular Article

INORGANIC CHEMISTRY RESEARCH
Published by the
Iranian Chemical Society
www.inorgchemres.org
info@inorgchemres.org

Inorg. Chem. Res., *Vol. 2, No. 2, 117-128, December 2019*
DOI: 10.22036/icr.2019.210340.1057

Platinum-oxygen Bond Formation: Kinetic and Mechanistic Studies

E. Haddadi[a], S.M. Nabavizadeh[a,*] and F. Niroomand Hosseini[b]

[a]*Professor Rashidi Laboratory of Organometallic Chemistry, Department of Chemistry, College of Sciences, Shiraz University, Shiraz, 71467-13565, Iran*

[b]*Department of Chemistry, Shiraz Branch, Islamic Azad University, Shiraz 71993-37635, Iran*

(Received 3 December 2019, Accepted 28 December 2019)

Reaction of [PtMe(C^N)(SMe_2)] (C^N = 2-phenylpyridinate (ppy); 1a, C^N = benzo[h]quinolate, (bhq); 1b) with hydrogen peroxide gives the platinum(IV) complexes *trans*-[PtMe($OH)_2$(C^N)(H_2O)] (C^N = ppy; 3a, C^N = bhq, 3b) bearing platinum-oxygen bonds. The Pt(II) complexes 1a and 1b have $5d_\pi$(Pt)→π*(C^N) MLCT band in the visible region which is used to easily follow the kinetic of its reaction with H_2O_2. The kinetics and mechanism of Pt-O bond formation have been experimentally and theoretically investigated, showing the simple second-order kinetics; rate = $k_2[H_2O_2]$[Pt(II) complex]. The Pt(IV) products were characterized by NMR spectroscopy and elemental analysis. The geometries and the nature of the frontier molecular orbitals of Pt(IV) complexes containing Pt-O bonds were also studied by means of the density functional theory. Complex 3b is unstable during the crystallization process in CH_2Cl_2/acetone and gives the binuclear complex [$Pt_2Me_2(Cl)_2(\mu$-$OH)_2(bhq)_2$], 4.

Keywords: Oxidative addition, Platinum, Kinetic and mechanism

INTRODUCTION

Oxidative addition reactions are one of the most popular types of organometallic reactions [1,2]. There are many reports on the activation of different substrates by Pt(II) d^8 organometallic complexes [3,4]. The contribution of these square-planar Pt(II) complexes in catalytic cycles is well known [5], for examples in the Shilov, Wacker, and Heck reactions [6-8]. Therefore, investigation of oxidative addition reactions of square-planar Pt(II) complexes have attracted significant interest in recent decades. The oxidative addition of different reagents to Pt(II) complexes resulting in the octahedral Pt(IV) compounds have been investigated by us and others [3,9-21].

There has been an increasing interest in antitumor activity of platinum compounds such as cisplatin, carboplatin and nedaplatin. A large number of Pt(II) and Pt(IV) complexes have been prepared to examine as antitumor agents and some of these compounds contain Pt-O bond [22,23]. The carboxylation of kinetically inert dihydroxoplatinum(IV) compounds with different substrates such as acid anhydrides and acyl chlorides to give bis(carboxylato)platinum(IV) complexes, as useful antitumor agents, has been of increasing interest [24]. One of the important route for making Pt-O bond is the oxidative addition of dioxygen or hydrogen peroxide to platinum complexes [25-27]. Reactions of organoplatinum(II) complexes with environmentally green oxidant, H_2O_2, have been studied [28,29]. Puddephatt and his coworkers prepared the complex [$Pt(OH)_2Me_2$(pyim)], pyim = 2-pyridyl-N-t-butylmethanimine, using oxidative addition of H_2O_2 to [$PtMe_2$(pyim)] [30]. The complex [$Pt(OH)_2Me_2$(pyim)] was unstable over a period of several hours to give the binuclear complex [$Pt_2Me_4(\mu$-$OH)_2(pyim)_2$]. The oxidative addition of H_2O_2 to [PtR_2(NN)], giving [$PtR_2(OH)_2$(NN)], where R = Me or Ar and NN = 2,2′-bipyridine (bpy) or 1,10-phenanthroline (phen) are also reported [31,32]. The oxygen-oxygen bond,

*Corresponding author. E-mail: nabavizadeh@shirazu.ac.ir

along with other Group 16-Group 16 bonds such as S-S or Se-Se are considered as non-polar or of low polarity substrate in the oxidative addition reactions [1,3]. The synthesis and characterization of Pt(IV) complexes [$PtR_2(SMe)_2(NN)$] (R = Me, *p*-MeC_6H_4 or *p*-$MeOC_6H_4$; NN = 2,2′-bipyridine (bpy), 4,4′-dimethyl-2,2′-bipyridine (dmbpy), 1,10-phenanthroline (phen) or 2,9-dimethyl-1,10-phenanthroline (dmphen)) has been studied [33]. Kinetics of the oxidative addition of some Group 16-Group 16 bonds to [$IrCl(CO)(PPh_3)_2$] has been studied and in each case a mechanism has been suggested [34,35].

Although, there are some reports on the preparation of Pt(IV)-O bonds by oxidation of Pt(II) complexes by hydrogen peroxide [28-30,32], the literature contains no report on kinetic and mechanistic study of the oxidative addition of this basic reagent to cycloplatinated(II) complexes. The purpose of the present work is to study the reactivity of some cycloplatinated(II) complexes towards hydrogen peroxide. The kinetic of the reaction including rate constants and activation parameters are determined and based on these data, a mechanism is suggested.

EXPERIMENTAL

^{1}H NMR spectra were recorded on a Varian 500 or 600 MHz spectrometer and referenced to the deuterated NMR solvents. All chemical shifts and coupling constants are given in ppm and Hz, respectively. The microanalyses were performed using a Thermofnigan Flash EA-1112 CHNSO rapid elemental analyzer. Melting points were recorded on a Buchi 530 apparatus. UV-Vis spectra and kinetics were recorded on a PerkinElmer Lambda 25 spectrophotometer with temperature control using an EYELA NCB-3100 constant-temperature bath. The starting cycloplatinated(II) complexes [$PtMe(ppy)(SMe_2)$], 1a, and [$PtMe(bhq)(SMe_2)$], 1b, were synthesized and characterized according to literature procedures [36,37]. NMR labeling is shown in Scheme 1.

Synthesis of Pt(IV) Complexes

***Trans*-[$PtMe(OH)_2(ppy)(H_2O)$], 3a.** [$PtMe(ppy)(SMe_2)$], 1a, (43 mg, 1 mmol), was dissolved in acetone or CH_2Cl_2 (15 ml) and H_2O_2 (1 ml, 9.8 M, 30%) was added to the solution. The mixture was stirred at room temperature over 30 min. The solvent was evaporated from the resulting pale yellow solution, and the residue was washed with ether and hexane. Yield: 86%. M. P.: 217 °C (decomp.). ^{1}H NMR in $CDCl_3$: δ 2.31 (s, ^{2}J(PtH) = 63.5 Hz, 3H, MePt), 7.18-7.26 (m, 3H), 6.74 (t, ^{3}J(HH) = 6.3 Hz, 1H, $H^{5'}$), 7.71 (d, ^{3}J(H^5H^4) = 7.19, 1H, H^5), 7.76 (t, ^{3}J(HH) = 7.61 Hz, 1H, H^4), 7.99 (d, 1H, ^{3}J(H^3H^4) = 8.13 Hz, H^3), 8.21 (d, ^{3}J(H^6H^5) = 4.91 Hz, 1H, H^6).

***Trans*-[$PtMe(OH)_2(bhq)(H_2O)$], 3b.** This compound was made similarly by using [$PtMe(bhq)(SMe_2)$], 1b, (45 mg, 1 mmol) and H_2O_2 (1 ml, 9.8 M, 30%). Yield: 81%. M. P.: 224 °C (decomp.). Anal. Calcd. for $C_{14}H_{15}NO_3Pt$: C, 38.19; H, 3.43; N, 3.18. Found: C, 37.95; H, 2.80; N, 3.05. ^{1}H NMR data in $CDCl_3$: δ 0.48 (b, 2H, OH groups), 2.59 (s, ^{2}J(PtH) = 64.9 Hz, 3H, MePt), 6.95 (dd, ^{3}J(H^3H^2) = 8.1 Hz, ^{3}J(H^3H^4) = 3.0 Hz, 1H, H^3), 7.49 (d, ^{3}J($H^{11}H^{10}$) = 7.5 Hz, 1H, H^{11}), 7.59 (t, ^{3}J(HH) = 7.5 Hz, 1H, H^{10}), 7.71 (d, ^{3}J(H^9H^{10}) = 7.4 Hz, 1H, H^9), 7.81 (d, ^{3}J(H^7H^6) = 8.9, 1H, $H^{6/7}$), 7.93 (d, 1H, ^{3}J(H^6H^7) = 8.7 Hz, $H^{6/7}$), 8.05 (dd, 1H, ^{3}J(H^4H^3) = 4.95 Hz, ^{4}J(H^2H^3) = 1.32 Hz, H^2), 8.27 (dd, 1H, ^{3}J(H^3H^4) = 8.4 Hz, H^4).

Kinetic Studies

For oxidative addition reactions of Pt(II) complexes with hydrogen peroxide, a solution of Pt(II) complex in acetone (3 ml, 3.0×10^{-4} M) in a cuvette was thermostated at 25 °C and a known excess of hydrogen peroxide was added to the solution. After rapid stirring, the absorbance at the corresponding wavelength (380 nm for complex 1a and 400 nm for complex 1b) was monitored over time. The absorbance-time profiles were analyzed using the equation $Abs_t = Abs_\infty + (Abs_0 - Abs_\infty) \exp(-k_{obs}.t)$ from which the observed first-order rate constants were obtained. A plot of k_{obs} *vs.* [H_2O_2] was linear and the slope gave the second-order rate constant. The data at other temperatures were obtained similarly and activation parameters were obtained from the Eyring equation (Eq. (1)).

$$\ln(\frac{k_2}{T}) = \ln(\frac{k_B}{h}) + \frac{\Delta S^{\mp}}{R} - \frac{\Delta H^{\mp}}{RT} \quad (1)$$

Crystallographic Data

Single crystal X-ray diffraction data of complex 4 was collected on a Bruker KAPPA APEX II diffractometer

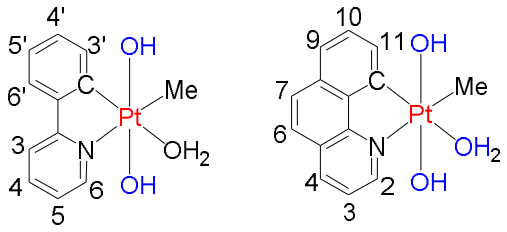

Scheme 1. NMR Labeling of Pt(IV) complexes

Table 1. Crystal Data and Structure Refinement for Complex 4.2$(CH_3)_2CO$

Empirical formula	$C_{34}H_{36}Cl_2N_2O_4Pt_2$	
Formula weight	997.73	
Temperature	100(2) K	
Wavelength	0.71073 Å	
Crystal system	Triclinic	
Space group	*P-1*	
Unit cell dimensions	a = 10.436(3) Å	α = 98.654(7)°
	b = 13.932(4) Å	β = 91.390(6)°
	c = 23.489(7) Å	γ = 100.130(6)°
Volume	3319.1(17) $Å^3$	
Z	4	
Density (calculated)	1.997 mg m^{-3}	
Absorption coefficient	8.621 mm^{-1}	
F(000)	1904	
Theta range for data collection	0.878-26.525°	
Reflections collected	19710	
Independent reflections	13318 [$R(int)$ = 0.0639]	
Max. and min. transmission	0.7454 and 0.6296	
Data/restraints/parameters	13318/0/607	
Goodness-of-fit on F^2	0.964	
Final R indices [I > 2sigma(I)]	$R1$ = 0.0576, $wR2$ = 0.0878	

equipped with an APEX II CCD detector using a TRIUMPH monochromator with a Mo *Kα* X-ray source (k = 0.71073 Å). The crystal was mounted on a cryoloop under Paratone-N oil and kept under nitrogen. Absorption correction of the data was carried out using the multiscan method SADABS [38]. Subsequent calculations were carried out using SHELXTL [39]. Structure determination was done using intrinsic methods. Structure solution, refinement, and creation of publication data was performed using SHELXTL. Crystallographic information is presented in Table 1. Crystallographic data for the structural analysis has been deposited with the Cambridge Crystallographic Data Centre, No. CCDC-1969119 Copies of this information may be obtained free of charge from: The Director, CCDC, 12 Union Road, Cambridge, CB2 1EZ, UK. Fax: +44(1223)336-033, e-mail: deposit@ccdc.cam.ac.uk, or www.ccdc.cam.ac.uk.

Computational Details

Gaussian 09 was used [40] to fully optimize all the structures at the B3LYP level of density functional theory. The effective core potential of Hay and Wadt with a double-ξ valence basis set (LANL2DZ) was chosen to describe Pt and I [41]. The 6-311++G** basis set was used for all other atoms. Frequency calculations were carried out at the same level of theory to identify whether the calculated stationary point is a minimum (zero imaginary frequency) or a transition-state structure (one imaginary frequency). All data were calculated at standard temperature and pressure (298.15 K and 1.0 atm). The solvation energies were calculated by CPCM model in acetone which reflect the operating experimental conditions.

RESULTS AND DISCUSSION

Synthesis and Characterization of the Organoplatinum(IV) Complexes

Hydrogen peroxide reacted cleanly with cycloplatinated(II) complexes [PtMe(C^N)(SMe_2)] (C^N = ppy, 1a; C^N = bhq, 1b) in dichloromethane or acetone at room temperature to give Pt(IV) complexes *trans*-[PtMe($OH)_2$(C^N)(SMe_2)] (C^N = ppy, 2a; C^N = bhq, 2b). The resulting Pt(IV) center absorbs H_2O to replace the SMe_2 ligand to form complexes *trans*-[PtMe($OH)_2$(C^N)(H_2O)] (C^N = ppy, 3a; C^N = bhq, 3b) which could be isolated as an air stable yellow solid. The reactions proceed by trans oxidative addition of HO-OH bond to platinum(II) complexes to give platinum(IV) complexes as shown in Scheme 2. Trans oxidative addition of the O-O bond is the usual stereochemistry of oxidative addition of H_2O_2 to Pt(II) complexes [31,42-45].

The ^{1}H NMR spectrum of 3b (Fig. 1) indicated methylplatinum group at δ 2.59, which was coupled with Pt to give satellites with ^{2}J(PtH) = 64.9 Hz, confirming that the methyl is directly bonded to platinum(IV). A broad resonance at δ 0.48 was assigned to the OH groups, since addition of D_2O led to loss of this peak and appearance of a peak due to HOD at δ 4.80 [46]. Inset of Fig. 1 shows the HH-COSY NMR of 3b, which was used to assign the aromatic hydrogens. The hydrogen related to the CH group adjacent to ligating N atom of the bhq ligand appeared as a doublet at δ 8.27 with J_{HH} = 8.4 Hz.

Attempts to grow crystals of Pt(IV) complexes for a single crystal X-ray diffraction experiment in solvents such as acetone and benzene were not successful. Complex 3b was unstable and decomposed over a period of several hours during crystallization process in CH_2Cl_2/acetone at room temperature. A reaction with solvent occurred to give the binuclear complex [$Pt_2Me_2(Cl)_2(\mu$-$OH)_2$(bhq)$_2$], 4 [47]. Complex 4 is characterized by structure determination. It crystallizes in the Triclinic crystal system in the space group *P-1*. Two crystallographically different but chemically identical complexes are located in the unit cell. The molecular structures and atom-numbering scheme of 4, as well as, selected bond distances and bond angles, are presented in Fig. 2. The crystallographic data and structure analysis of complex 4 are summarized in Table 1. Each platinum(IV) center has octahedral stereochemistry with a chelating bhq ligand, one methyl, one Cl and two bridging OH groups. As expected, the bhq ligand binds to the Pt(IV) center via one N and one C atom. Two C coordinated atoms (C of bhq and C of Me) take cis positions. The angles around the Pt center deviate significantly from 90°, *i.e.* the (bhq) bite angles, C(12)-Pt(1)-N(1) and C(26)-Pt(2)-N(2) are reduced to 82.6(4)° and 81.8(4)°, respectively, implying that the chelate is probably under strain, whereas the angles formed by the Me ligand with the O atom of OH, *i.e.* C(1)-Pt(1)-O(1) and Cl ligand with O atom, *i.e.* O(2)-Pt(1)-Cl(1)

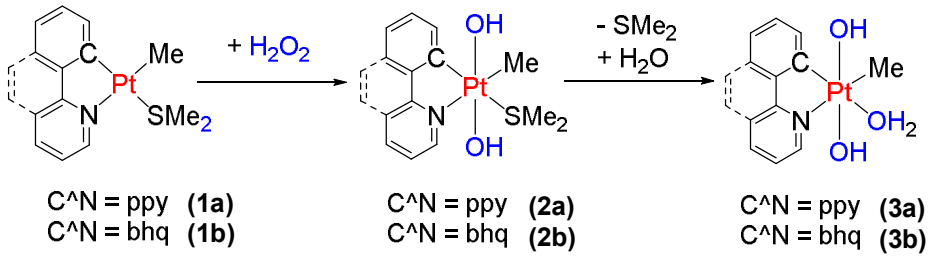

Scheme 2. Platinum-oxygen bond formation by oxidative addition of H_2O_2 to Pt(II) complexes

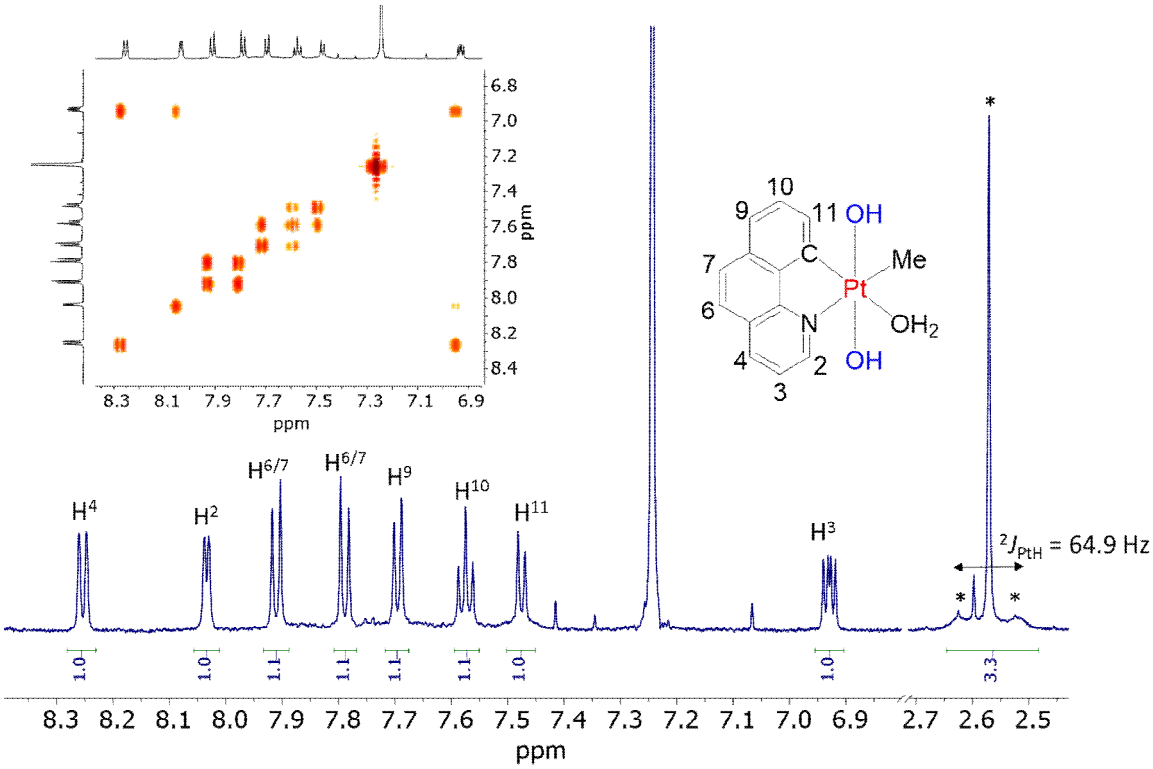

Fig. 1. ^{1}H NMR of complex 3b in $CDCl_3$. The inset shows HH-COSY NMR in the aromatic region.

are increased to 92.6(4)° and 96.9(2)°, respectively. The PtOH groups in 4 involved in hydrogen bonding to solvate acetone molecules between oxygen atom of acetone and hydrogen of PtOH group. The intramolecular Pt-Pt distance is 3.2394(11) Å which indicates weak interactions between two Pt centers in solid state. This Pt-Pt distance is very close to the value of 3.230 Å reported for Pt-Pt distance in an analog hydroxo bridged complex [$Pt_2Me_4(\mu$-OH)$_2$(picolinate)$_2$] [30].

Kinetic Studies of the Oxidative Addition Reaction of Pt(II) Complexes with Hydrogen Peroxide

The oxidative addition reaction of Pt(II) complexes with hydrogen peroxide was investigated by using UV-Vis spectroscopy. A known excess of H_2O_2 was added to a solution of Pt(II) complex and disappearance of the MLCT band at the corresponding λ_{max} was used to monitor the reaction. Changes in the spectrum during a typical run are shown in Fig. 3. The absorbance-time profiles were

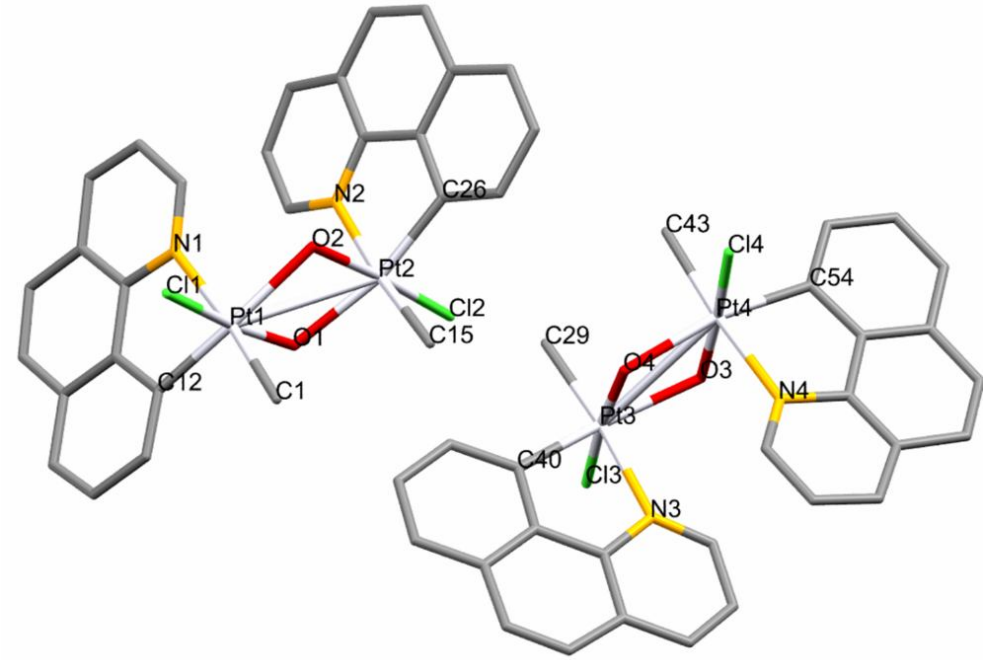

Fig. 2. Crystal structure of complex 4. The H atoms and solvents are omitted for clarity. Selected bond distance (Å) and angles (°): C(1)-Pt(1) 2.026(11); C(15)-Pt(2) 2.038(11); C(26)-Pt(2) 1.989(12); Cl(1)-Pt(1) 2.315(3); Cl(2)-Pt(2) 2.301(3); N(1)-Pt(1) 2.145(9); N(2)-Pt(2) 2.149(10); O(1)-Pt(1) 2.027(7); O(2)-Pt(1) 2.184(8); Pt(1)-Pt(2) 3.2394(11); C(12)-Pt(1)-C(1) 92.7(5); C(12)-Pt(1)-O(1) 91.4(4); C(1)-Pt(1)-O(1) 92.6(4); C(12)-Pt(1)-N(1) 82.6(4); C(1)-Pt(1)-N(1) 174.9(5); O(1)-Pt(1)-N(1) 89.6(3); C(12)-Pt(1)-O(2) 165.7(4); C(1)-Pt(1)-O(2) 97.1(4); O(1)-Pt(1)-O(2) 77.8(3); N(1)-Pt(1)-O(2) 87.9(3); C(12)-Pt(1)-Cl(1) 93.8(3); C(1)-Pt(1)-Cl(1) 87.8(4); O(1)-Pt(1)-Cl(1) 174.8(2); N(1)-Pt(1)-Cl(1) 90.4(2); O(2)-Pt(1)-Cl(1) 96.9(2); C(12)-Pt(1)-Pt(2) 132.1(3); C(1)-Pt(1)-Pt(2) 91.8(4); O(1)-Pt(1)-Pt(2) 40.7(2); N(1)-Pt(1)-Pt(2) 92.8(3); O(2)-Pt(1)-Pt(2) 37.55(19); Cl(1)-Pt(1)-Pt(2) 134.06(8); C(26)-Pt(2)-C(15) 93.8(5); C(26)-Pt(2)-N(2) 81.8(4); C(15)-Pt(2)-N(2) 175.1(5); C(26)-Pt(2)-Cl(2) 92.9(3); C(15)-Pt(2)-Cl(2) 88.8(4); N(2)-Pt(2)-Cl(2) 89.2(3).

Table 2. Rate Constants and Activation Parameters for Reaction of Pt(II) Complexes with H_2O_2 in Acetone

		Rate constants at different temperatures				$\Delta H^{\ddagger}$	$\Delta S^{\ddagger}$
		5 °C	15 °C	25 °C	30 °C	(kcal mol^{-1})	(cal K^{-1} mol^{-1})
1a	k_1 (s^{-1})	0.08	0.06	0.23	0.61		
	k_2 (M^{-1} s^{-1})	0.66	1.22	3.11	3.40	11.1 ± 0.6	-13 ± 2
1b	k_1 (s^{-1})	0.05	0.00	0.00	0.21		
	k_2 (M^{-1} s^{-1})	0.48	1.27	3.81	4.67	15.3 ± 0.5	1 ± 2

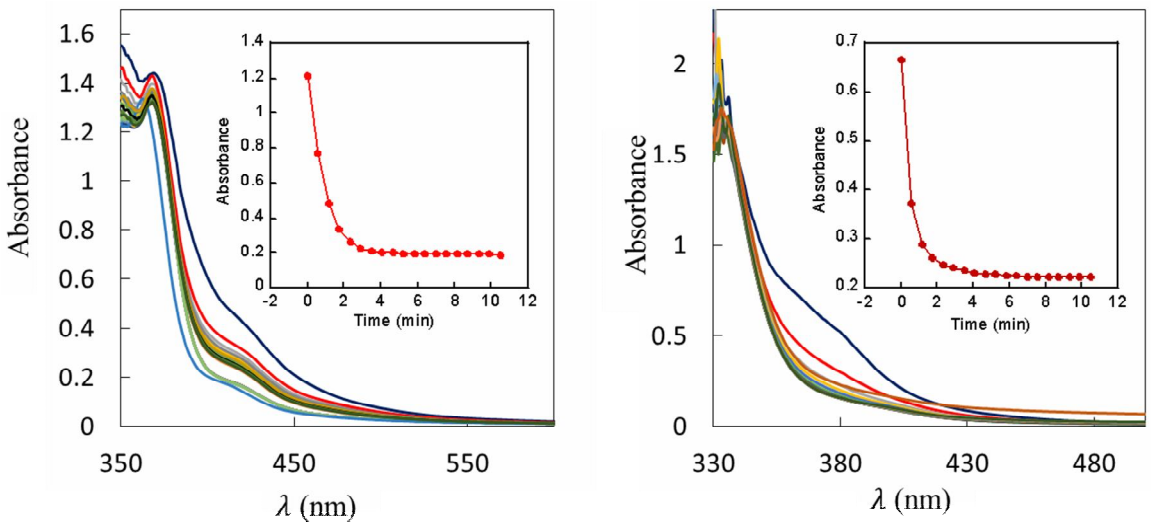

Fig. 3. Changes in the UV-Vis spectrum during the reaction of [PtMe(bhq)(SMe_2)] (left) (6×10^{-4} M) or [PtMe(ppy)(SMe_2)] (right) (1×10^{-3} M) in acetone at $T = 25$ °C. Successive spectra were recorded at intervals of 30 s; the inset shows the analysis of the spectrophotometric data to evaluate the pseudo-first order rate constant according to $Abs_t = Abs_\infty + (Abs_0 - Abs_\infty) \exp(-k_{obs}.t)$.

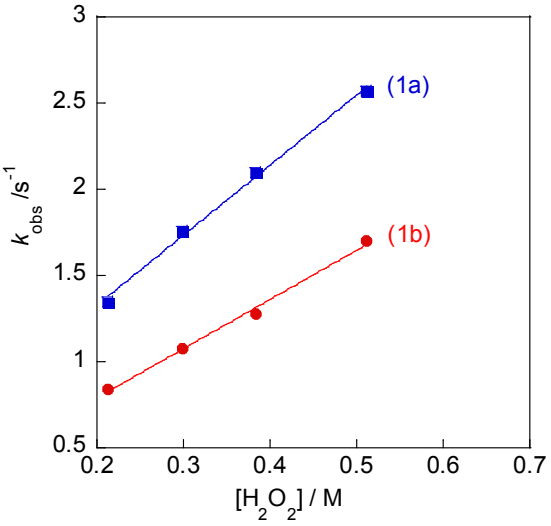

Fig. 4. Plots of pseudo first-order rate constants for the reaction of complexes 1a and 1b with H_2O_2 at 25 °C *vs.* [H_2O_2] in acetone.

analyzed using the pseudo first-order equation, $Abs_t = Abs_\infty + (Abs_0 - Abs_\infty) \exp(-k_{obs}.t)$. The experimentally determined pseudo-first-order rate constant, k_{obs}, was converted to second order rate constant (k_2) by determining slope of the linear plots of k_{obs} against [H_2O_2] according to equation $k_{obs} = k_1 + k_2$ [H_2O_2] (see Fig. 4). The second-order terms, k_2, is suggested for the simple associative S_N2-type mechanism and a much smaller term, k_1, is described for associative substitutions by acetone solvent. The results are given in Table 2. The findings are consistent with the reaction

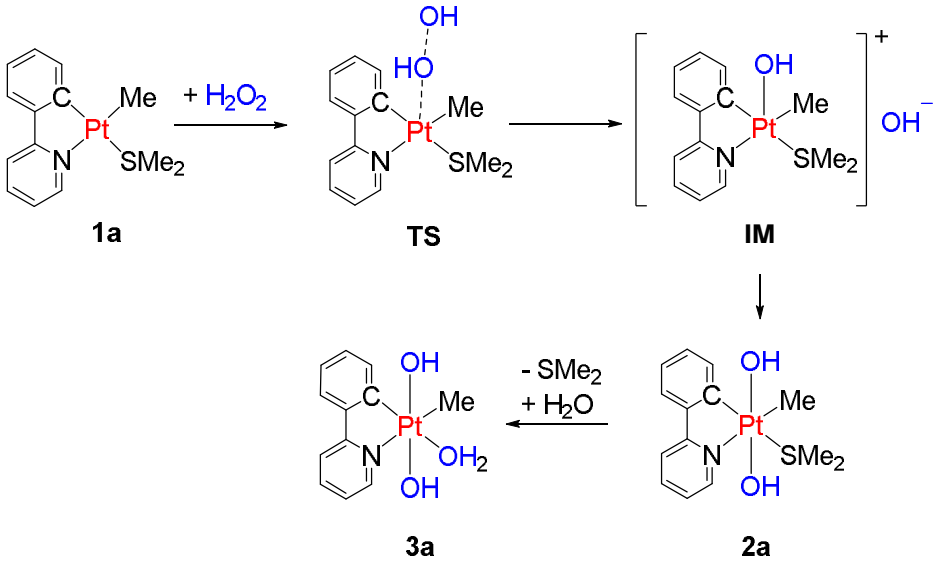

Scheme 3. Suggested mechanism for the oxidative addition reaction of Pt(II) complex with H_2O_2

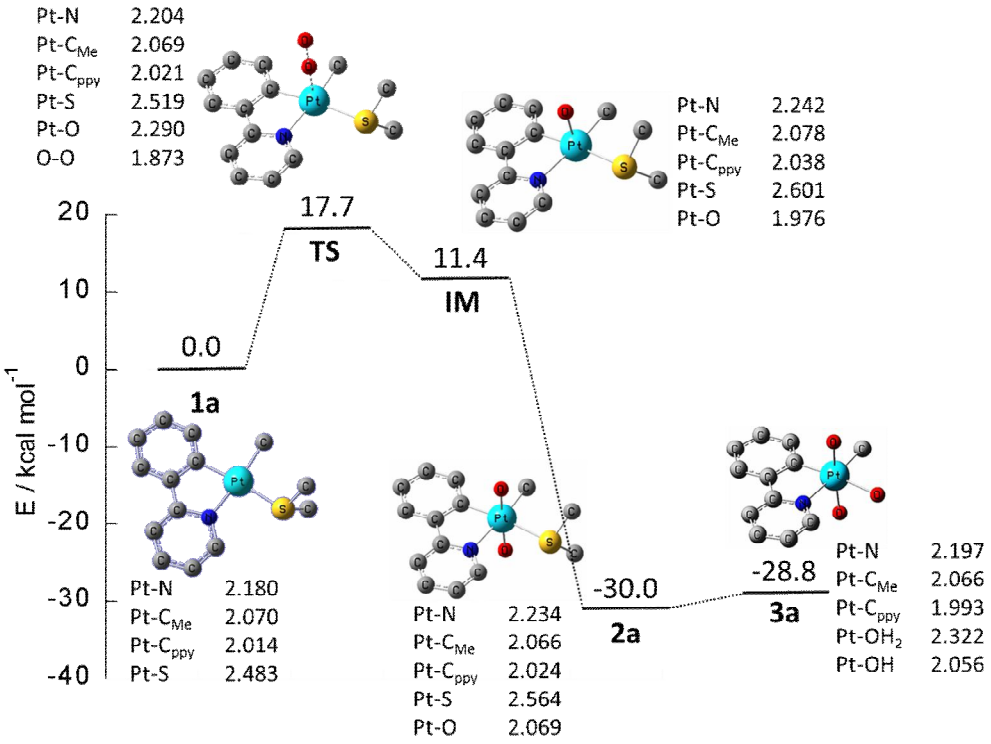

Fig. 5. Energy profile for oxidative addition of H_2O_2 to [PtMe(ppy)(SMe_2)], 1a, in acetone. The H atoms were removed for clarity. Selected bond lengths (Å) are also shown.

mechanism shown in Scheme 3 for reaction of Pt(II) complex with H_2O_2. The values of $\Delta S^{\ddagger}$ in each reaction indicate that an association has taken place in the transition state. On the basis of experimental findings, a mechanism, shown in Scheme 3, is suggested for the reaction of Pt(II) complexes with hydrogen peroxide. The reaction proceeds through an S_N2-type mechanism by nucleophilic attack of the platinum atom of 1a on the oxygen in hydrogen peroxide, to afford the cationic platinum(IV) intermediate, IM, through the transition state TS. Next, the free hydroxo ion coordinates to the platinum(IV) center of $[PtMe(OH)(C^N)(SMe_2)]^+$ cationic intermediate to form the dihydroxo platinum(IV), *trans*-$[PtMe(OH)_2(C^N)(SMe_2)]$. Finally, resulting Pt(IV) center probably absorbs H_2O (from moisture) to replace the SMe_2 ligand and give final product 3a.

DFT Calculations

To shed some light on the suggested mechanism (depicted in Scheme 1), DFT calculations were carried out on the precursor complex 1a, final product 3a, and potential transition state and intermediate. The Conductor like Polarizable Continuum Model (CPCM) was used to model general solvation effects by acetone. The reaction is initiated by attacking the Pt atom of Pt(II) complex 1a onto the oxygen atom of H_2O_2. Substitution of a hydroxo group by the Pt center, followed by simultaneous partial removal of a hydroxo ion, results in formation of the transition state TS (Fig. 6). The free energy barrier for this step was calculated to be 17.7 kcal mol^{-1} in acetone at 298.15 K, which is in excellent agreement with the experimental value of 15.0 kcal mol^{-1}. In TS, the bond angle Pt-O-O is equal to 178.6°, showing a linear arrangement with the hydroxo group. During the formation of TS, the most significant changes in bond distances are observed for Pt-O and O-O distances. The O-O bond length increases from 1.451 Å in H_2O_2 to 1.873 Å in TS, whereas the Pt-O distance decreases from far apart in the reactant to 2.290 Å in TS. This confirms that oxidative addition of H_2O_2 to 1a involves simultaneous cleavage of O-O bond and formation of Pt-O bond, which is followed by formation of the cationic intermediate IM by completely breaking and forming of the O-O and Pt-O bonds, respectively. The intermediate IM has a square pyramidal geometry around Pt, with the incoming OH group occupying the apical position and the other OH ion being in the outer sphere of IM. The coordination of OH ion to the platinum center gives complex 2a. The latter can absorb water to form cycloplatinated(IV) complex 3a by replacement of SMe_2 by H_2O. Product 3a has an octahedral geometry around the Pt(IV) center (see Fig. 5) with Pt-OH bond length of 2.056 Å in excellent agreement with the experimental x-ray value of 2.027(7) Å for similar complex $[PtCl(OH)(CH_2CMe_2C_6H_4)(NN)]$, where NN = 3,4,7,8-tetramethyl-1,10-phenanthroline [42].

The contours and energies of several highest occupied molecular orbitals (HOMOs) and lowest unoccupied molecular orbitals (LUMOs) for the starting Pt complex 1a, TS, 2a and final Pt(IV) product 3a are shown in Fig. 6. Analysis of the frontier molecular orbitals for complex 1a reveals that the maximum contributions to HOMO and HOMO-1 belong to the Pt metal center with a small contribution of cyclometalated ligand (ppy). These calculations further show that LUMO and LUMO+1 of 1a are significantly localized on the ppy cyclometalated ligand. At the end of reaction and after oxidative addition reaction and replacement of SMe_2 by H_2O, the complex 3a is formed in which the frontier orbitals are localized on Pt and OH groups (for HOMO) and ppy ligand (for LUMO). Comparing the HOMOs of 1a and 3a shows the moving of electron density from Pt(II) center in 1a to OH groups in 3a due to oxidation process. As shown in Fig. 7, main contribution to Pt-O in the transition state TS comes from overlap of HOMO of the platinum center with the LUMO of H_2O_2. So it is reasonable to view the oxidation process formally as removal of electrons from HOMO of 1a into the LUMO of H_2O_2.

CONCLUSIONS

In conclusion, we have shown that the reaction of H_2O_2 with cycloplatinated(II) complexes results in exclusive formation of the trans-dihydroxo cycloplatinated(IV) complexes. During the crystallization process, a reaction with solvent was observed, resulting in the formation of a binuclear cycloplatinated(IV) complex containing hydroxo groups as bridging ligands. As supported by experimental and theoretical investigations, oxidative addition reaction of H_2O_2 with the Pt(II) complexes occurs *via* S_N2 mechanism.

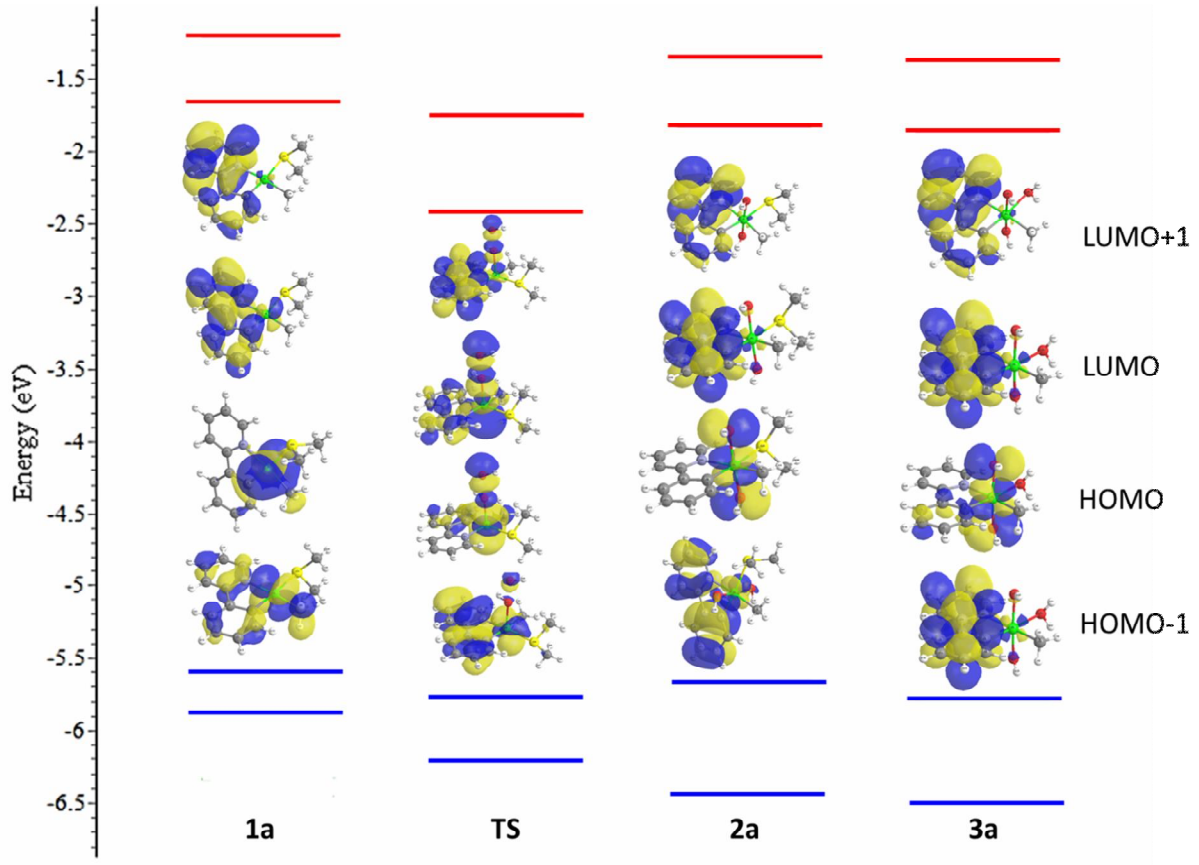

Fig. 6. Qualitative frontier molecular orbital scheme for 1a, TS, 2a and 3a.

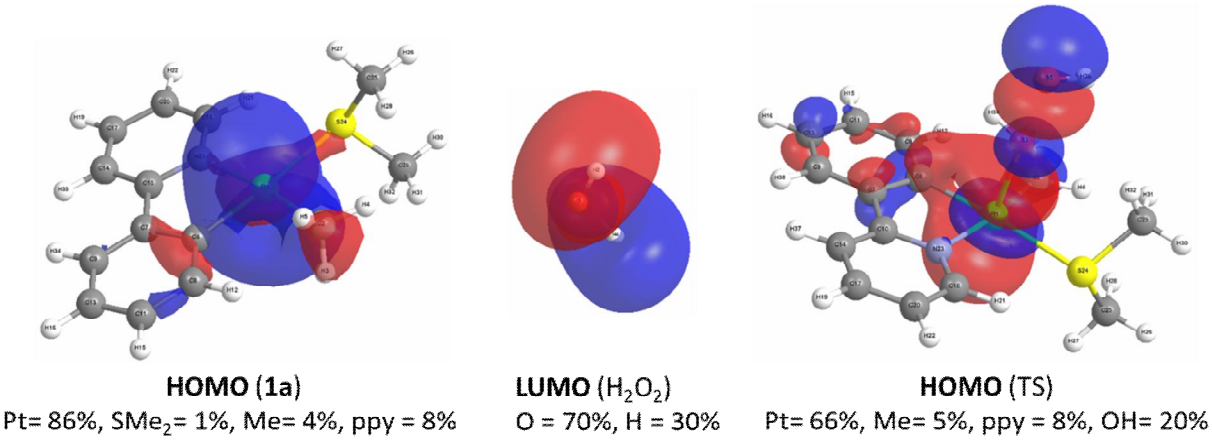

Fig. 7. HOMO, LUMO and HOMO of 1a, H_2O_2 and TS, respectively.

REFERENCES

[1] J.P. Collman, Priciples and Applications of Organotransition Metal Chemistry, University Science Books, 1987.

[2] S.G. Davies, Organotransition Metal Chemistry: Applications to Organic Synthesis: Applications to Organic Synthesis, Elsevier, 2013.

[3] L.M. Rendina, R.J. Puddephatt, Chem. Rev. 97 (1997) 1735.

[4] M. Crespo, M. Martinez, S.M. Nabavizadeh, M. Rashidi, Coord. Chem. Rev. 279 (2014) 115.

[5] P.J. Craig, R. Jenkins, in Organic Metal and Metalloid Species in the Environment, Springer, 2004, pp. 1-15.

[6] J.F. Hartwig, Nature 455 (2008) 314.

[7] J.A. Labinger, J.E. Bercaw, Nature 417 (2002) 507.

[8] A.E. Shilov, G.B. Shul'pin, Chem. Rev. 97 (1997) 2879.

[9] S.M. Nabavizadeh, S.J. Hoseini, B.Z. Momeni, N. Shahabadi, M. Rashidi, A.H. Pakiari, K. Eskandari, Dalton Trans. (2008) 2414.

[10] S.M. Nabavizadeh, E.S. Tabei, F.N. Hosseini, N. Keshavarz, S. Jamali, M. Rashidi, New J. Chem. 34 (2010) 495.

[11] S.M. Nabavizadeh, H.R. Shahsavari, H. Sepehrpour, F.N. Hosseini, S. Jamali, M. Rashidi, Dalton Trans. 39 (2010) 7800.

[12] C.M. Anderson, R.J. Puddephatt, G. Ferguson, A.J. Lough, J. Chem. Soc. Chem. Commun. (1989) 1297.

[13] C. Anderson, M. Crespo, Organometallics 10 (1991) 2672.

[14] M. Rashidi, S.M. Nabavizadeh, A. Akbari, S. Habibzadeh, Organometallics 24 (2005) 2528.

[15] S.M. Nabavizadeh, S. Habibzadeh, M. Rashidi, R.J. Puddephatt, Organometallics 29 (2010) 6359.

[16] N.H. Fatemeh, Z. Farasat, S.M. Nabavizadeh, G. Wu, M.M. Abu-Omar, J. Organomet. Chem. 880 (2019) 232.

[17] P. Hamidizadeh, S.M. Nabavizadeh, S.J. Hoseini, Dalton Trans. 48 (2019) 3422.

[18] M.D. Aseman, S.M. Nabavizadeh, F. Niroomand Hosseini, G. Wu, M.M. Abu-Omar, Organometallics 37 (2018) 87.

[19] F. Niroomand Hosseini, S.M. Nabavizadeh, M.M. Abu-Omar, Inorg. Chem. 56 (2017) 14706.

[20] S. Chamyani, H.R. Shahsavari, S. Abedanzadeh, M. Golbon Haghighi, S. Shabani, B. Notash, Appl. Organomet. Chem. 33 (2019) e4674.

[21] F. Niroomand Hosseini, Inorg. Chem. Res. 2 (2019) 26.

[22] A. Kritchenkov, Y.M. Stanishevskii, Y.A. Skorik, Pharm. Chem. J. 53 (2019) 6.

[23] N. El Brahmi, S.M. Mignani, J. Caron, S. El Kazzouli, M.M. Bousmina, A.-M. Caminade, T. Cresteil, J.-P. Majoral, Nanoscale 7 (2015) 3915.

[24] S. Choi, C. Filotto, M. Bisanzo, S. Delaney, D. Lagasee, J.L. Whitworth, A. Jusko, C. Li, N. A. Wood, J. Willingham, Inorg. Chem. 37 (1998) 2500.

[25] D. Watts, D. Wang, M. Adelberg, P.Y. Zavalij, A.N. Vedernikov, Organometallics 36 (2016) 207.

[26] A.R. Petersen, A.J. White, G.J. Britovsek, Dalton Trans. 45 (2016) 14520.

[27] M. Azizpoor Fard, A. Behnia, R.J. Puddephatt, Organometallics 36 (2017) 4169.

[28] A.N. Vedernikov, Acc. Chem. Res. 45 (2011) 803.

[29] E.M. Prokopchuk, H.A. Jenkins, R.J. Puddephatt, Organometallics 18 (1999) 2861.

[30] N. Nasser, M.A. Fard, P.D. Boyle, R.J. Puddephatt, J. Organomet. Chem. 858 (2018) 67.

[31] K.-T. Aye, J.J. Vittal, R.J. Puddephatt, J. Chem. Soc. Dalton Trans. (1993) 1835.

[32] M. Rashidi, M. Nabavizadeh, R. Hakimelahi, S. Jamali, J. Chem. Soc. Dalton Trans. (2001) 3430.

[33] F.N. Hosseini, M. Rashidi, S.M. Nabavizadeh, J. Mol. Struc. 1125 (2016) 20.

[34] C.T. Lam, C.V. Senoff, Can. J. Chem. 51 (1973) 3790.

[35] R.T. Mehdi, J.D. Miller, J. Chem. Soc. Dalton Trans. (1984) 1065.

[36] J.S. Owen, J.A. Labinger, J.E. Bercaw, J. Am. Chem. Soc. 126 (2004) 8247.

[37] S.M. Nabavizadeh, M.G. Haghighi, A.R. Esmaeilbeig, F. Raoof, Z. Mandegani, S. Jamali, M. Rashidi, R.J. Puddephatt, Organometallics 29 (2010) 4893.

[38] G. Sheldrick, SADABS, Empirical Absorption Correction Program; University of Göttingen: Germany, 1997, 2005.

[39] SHELXTL PC, Version 6.12, Bruker AXS Inc.,

Madison, WI, 2005.

[40] M. Frisch, G. Trucks, H. Schlegel, G. Scuseria, M. Robb, J. Cheeseman, G. Scalmani, V. Barone, B. Mennucci, G. Petersson, Gaussian 09, Revision A. 02; Gaussian, Inc: Wallingford, CT, 2009

[41] P.J. Hay, W.R. Wadt, J. Chem. Phys. 82 (1985) 270.

[42] M.A. Fard, A. Behnia, R.J. Puddephatt, J. Organomet. Chem. 890 (2019) 32.

[43] V.V. Rostovtsev, L.M. Henling, J.A. Labinger, J.E. Bercaw, Inorg. Chem. 41 (2002) 3608.

[44] K. Thorshaug, I. Fjeldahl, C. Rømming, M. Tilset, Dalton Trans. (2003) 4051.

[45] F. Zhang, E.M. Prokopchuk, M.E. Broczkowski, M.C. Jennings, R.J. Puddephatt, Organometallics 25 (2006) 1583.

[46] G.R. Fulmer, A.J. Miller, N.H. Sherden, H.E. Gottlieb, A. Nudelman, B.M. Stoltz, J.E. Bercaw, K.I. Goldberg, Organometallics 29 (2010) 2176.

[47] L.A. Wickramasinghe, P.R. Sharp, Inorg. Chem. 53 (2014) 1430.